

# Structure—Activity Relationship Studies To Probe the Phosphoprotein Binding Site on the Carboxy Terminal Domains of the Breast Cancer Susceptibility Gene 1

Ziyan Yuan,<sup>†,§</sup> Eric A. Kumar,<sup>†,§</sup> Smitha Kizhake,<sup>†,§</sup> and Amarnath Natarajan<sup>\*,†,§</sup><sup>†</sup>Eppley Institute for Cancer Research and Allied Diseases, and <sup>‡</sup>Department of Genetics Cell Biology and Anatomy, University of Nebraska Medical Center, Omaha, Nebraska 68198, United States<sup>§</sup>Chemical Biology Program, Department of Pharmacology, University of Texas Medical Branch, Galveston, Texas 77555, United States Supporting Information

**ABSTRACT:** Carboxy terminal BRCT domains of the breast cancer susceptibility gene 1 (BRCA1) bind to phosphorylated proteins through a pSXXF consensus recognition motif. We report a systematic structure—activity relationship study that maps the BRCT(BRCA1)—pSXXF binding interface, leading to identification of peptides with nanomolar binding affinities comparable to those of the previously reported 13-mer peptides and providing a clear description of the pSXXF—BRCT interface, which is essential for developing small molecule inhibitors via the peptidomimetic approach.

## INTRODUCTION

Protein—protein interactions are the driving force that underlies multiple signaling events and the corresponding cellular functions. Because of the transient nature of these interactions, classical biochemical techniques are limited in their ability to precisely and temporally perturb these systems. Chemical probes are emerging as a viable alternative to dissect complex networks of protein—protein interactions.<sup>1</sup> Recently, high-throughput screening (HTS) has been used to identify chemical probes for protein—protein interactions.<sup>2,3</sup> Current methodologies result in low hit rates and weak affinities which suggest the need for development of alternative approaches. The rational design of peptidomimetics starting from a small peptide with low micromolar affinities which can be used to overcome the shortcomings of HTS.<sup>4,5</sup>

The tumor suppressor protein BRCA1 maintains the integrity of the genome by mediating DNA damage response.<sup>6</sup> The carboxy terminal domains of BRCA1 (BRCT) recognize and bind phosphorylated protein partners in response to DNA damage, such as Abraxas and BACH1.<sup>7,8</sup> The interactions of BRCT and phosphorylated proteins are mediated through a pSXXF consensus recognition motif. The BRCT(BRCA1)—pSXXF interaction is anchored through a two-point binding mode: a hydrophilic contact made by the phosphorylated serine (pS) residue and a hydrophobic contact made by the phenylalanine (F) residue.<sup>9–14</sup>

Reproducible fluorescence polarization (FP) assays were developed to dissect BRCT—phosphoproteins interaction and identify small molecules that will specifically bind to the pSXXF binding site on BRCT.<sup>15,16</sup> Tetrapeptides that bind BRCT with micromolar affinities were identified using FP assays.<sup>17</sup> These tetrapeptides bind to the BRCT at the exact same site as the 13-mer peptides (ISRSTpSPTFNKQT) previously reported.<sup>18,19</sup> A combination of orthogonal techniques, FP and Isothermal titration calorimetry (ITC), was used in this study to determine the structure—activity relationship (SAR), and the enthalpic and

entropic contributions associated with the BRCT—tetrapeptide interactions were modeled using a thermodynamic optimization plot (TOP).<sup>20</sup> These studies resulted in the identification of peptide **18** (Ac-pSPTF-CO<sub>2</sub>H) with nanomolar binding affinity for BRCT(BRCA1).

## RESULTS AND DISCUSSION

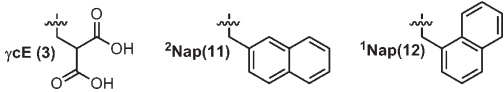
IC<sub>50</sub> values obtained from the screen are summarized in Table 1. A SAR of BRCT—tetrapeptide was constructed, and the structural basis is shown in Figure 1.

**Modification to the pS (P Position) Residue.** Peptides **2–4** containing phosphoserine mimics were used to explore the phosphate-binding site. Previously, our laboratory has shown that substituting the phosphoserine mimic using glutamate (E) into the peptide sequence renders it inactive.<sup>17</sup> Structural studies showed that the three oxygen atoms on the phosphate group are in proximity to the side chains of Lys<sub>1702</sub>, Ser<sub>1655</sub>, and the amide nitrogen of Gly<sub>1656</sub> on the N-terminus BRCT domain.<sup>9–14</sup> Consistent with this observation, peptide **3** containing a  $\gamma$ -carboxyglutamate ( $\gamma$ cE) side chain with four oxygen atoms and two OH groups resulted in a partial rescue of the inhibitory activity (compared to **2**), confirming that at least three heteroatoms are needed to make the hydrophilic contacts. The phosphothreonine (pT) peptide **4** was used to explore the size of the phosphate-binding site. Remarkably, this peptide was inactive. Analysis of the crystal structure reveals that rotation of the C <sub>$\alpha$</sub> —C <sub>$\beta$</sub>  bond on pT could minimize the steric interaction (Figure 1A; see arrow) between the methyl group on pT and the Thr<sub>1700</sub> side chain on BRCT. This conformational change will force the phosphate group on pT to orient away from the hydrophilic contacts on BRCT, resulting in the loss of activity.

Received: December 25, 2010

Published: May 16, 2011

Table 1. SAR of Tetrapeptides



compd	peptide	IC <sub>50</sub> (μM)
1	Ac-pSPTF-CONH <sub>2</sub>	4.6 ± 0.9
2	Ac-EPTF-CONH <sub>2</sub>	>250
3	Ac-γcEPTF-CONH <sub>2</sub>	52.8 ± 1.6
4	Ac-pTPTF-CONH <sub>2</sub>	>250
5	Ac-pSATF-CONH <sub>2</sub>	15.0 ± 1.7
6	Ac-pSPAF-CONH <sub>2</sub>	35.0 ± 7.9
7	Ac-pSPVF-CONH <sub>2</sub>	3.2 ± 0.8
8	Ac-pSPSF-CONH <sub>2</sub>	30.1 ± 7.2
9	Ac-pSPIF-CONH <sub>2</sub>	7.1 ± 1.4
10	Ac-pSPLF-CONH <sub>2</sub>	18.4 ± 1.8
11	Ac-pSPT <sup>2</sup> Nap-CONH <sub>2</sub>	17.7 ± 2.3
12	Ac-pSPT <sup>1</sup> Nap-CONH <sub>2</sub>	171.7 ± 10.2
13	Ac-pSPTY-CONH <sub>2</sub>	14.9 ± 2.8
14	Ac-pSAAF-CONH <sub>2</sub>	98.4 ± 23.1
15	Ac-pSPPF-CONH <sub>2</sub>	>250
16	Ac-FTApS-CONH <sub>2</sub> (all D amino acids)	>250
17	H-pSPTF-CONH <sub>2</sub>	10.8 ± 1.4
18	Ac-pSPTF-COOH	1.0 ± 0.2
19	Ac-pSPVF-COOH	1.6 ± 0.3

**Modification to the P + 1 Residue.** The role of the Pro residue in pSPTF binding to BRCT was investigated using the pSATF peptide **5**. This modification resulted in a ~3-fold loss of activity compared to the parent peptide **1**. This suggests that the Pro residue is critical in restricting the peptide to the bound conformation.

**Modification to the P + 2 Residue.** Peptides **6–10** with systematic changes to the P + 2 positions were used to explore the role of (a) OH on the side chain and (b) steric interaction by the β-branching on the Thr (T) side chain. Interestingly, compared to the peptide **1**, the Ala substituted peptide **6** and the Ser substituted peptide **8** resulted in ~7-fold loss of activity, while the Val substituted peptide **7** showed slightly improved activity. This result indicates that the steric interaction is more important than the OH functionality.

Peptides with the isopentane side chains, the Ile substituted peptide **9** and the Leu substituted peptide **10**, which are β and γ branched, respectively, were screened to further explore this steric interaction. Both peptides were less active compared to peptides **1** and **7** with the Thr/Val side chains. Note that peptide **9** with the β-branching is more active than peptide **10** with γ-branching. Together, the SAR at the P + 2 position clearly shows that β-branched peptides (**1**, **7**, and **9**) are ~3- to 8-fold more active than unbranched (**6** and **8**) or γ-branched (**10**) peptides. This analysis and examination of the crystal structure reveal that the steric interaction with the side chain of Glu<sub>1698</sub> on BRCT contributes to the BRCT–peptide interaction and that β-branching is optimal at this position (Figure 1B).

**Modification to the P + 3 Residue.** Peptides **11** and **12** were synthesized to incorporate unnatural amino acids with naphthyl side chains (<sup>1</sup>Nap and <sup>2</sup>Nap) to explore the size and shape of the

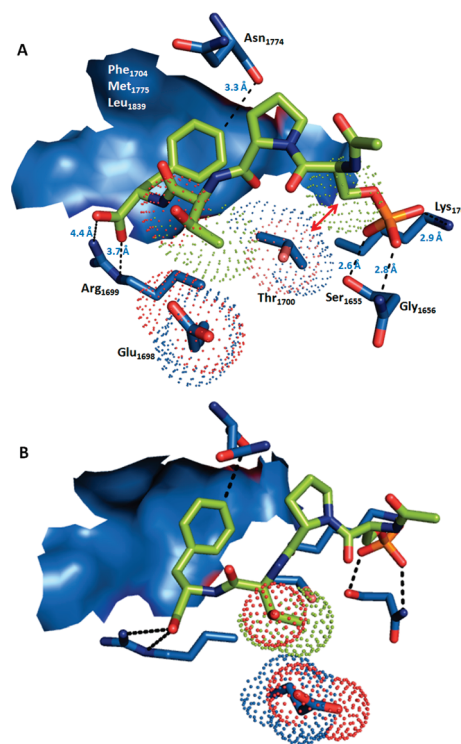


**Figure 1.** (A, B) Two orientations of the pSPTF–BRCT(BRCA1) binding interface. The tetrapeptide is shown as green sticks, while the protein is shown in blue. The potential hydrophilic contacts are shown by broken dotted lines, and the hydrophobic contacts are shown as surface or by dots. The red double headed arrow shows the contact made by the β-carbon on pSer with the Thr<sub>1700</sub> side chain on BRCT (PDB code 1T29).

hydrophobic patch. Both modifications resulted in partial loss of activity (Table 1); however, the <sup>2</sup>Nap substitution is an order of magnitude better than the <sup>1</sup>Nap substitution. This change suggests that the Phe binding pocket is asymmetric and will better accommodate substitution at the para position on the phenyl ring compared to the ortho position. The Tyr containing peptide **13** was used to explore the effect of para substitution and possible hydrogen bonding with the amide carbonyl of Asn<sub>1774</sub> on BRCT. This substitution, however, resulted in a 3-fold loss of activity and suggests that this pocket does not tolerate even small extensions to the phenyl ring.

**Combinatorial Effects.** The pSATF peptide **5** and the pSPAF peptide **6** are ~3-fold and ~7.5-fold less active than **1**, respectively. Remarkably, the pSAAF peptide **14** with the combined substitution is ~21-fold less active than **1**. This result highlights that the interactions made by the middle residues are linked and contribute to the overall binding in a combinatorial manner.

**Modification to the pSXXF Backbone.** Peptides **15** and **16** were synthesized to explore the contribution of the backbone to BRCT–peptide binding. It is known that proline dimers tend to adopt the polyproline type II (PPII) secondary structure because of minimization of the pseudo allylic (1,3) strain (see Supporting Information Figure S1).<sup>21</sup> The PPII secondary structure is defined by the backbone dihedral angles  $\varphi_{\text{CO-N-C}\alpha\text{-CO}} = -75^\circ$ ,  $\psi_{\text{N-C}\alpha\text{-CO-N}} = +145^\circ$ . Peptides containing Pro-Pro motifs will adopt the PPII conformation and, therefore will be conformationally constrained, resulting in rigid scaffolds.<sup>22</sup> The pSPPF peptide **15**, wherein a Pro-Pro motif is

introduced, was used to explore this effect. This modification resulted in >50-fold loss of activity compared to the parent peptide **1**, suggesting that rigidifying the pSXXF peptide to the PPII conformation is not favorable.

Reversing the peptide sequence, combined with D amino acids, is a common approach used to stabilize peptides to cellular degradation.<sup>23</sup> The reversed-sequence peptide will have the amide bonds reversed, but the side chains will orient similar to the parent L-peptide. To test the effect in our system, we generated peptide **16** which has the side chains positioned correctly to facilitate optimum contact with the protein (see Supporting Information Figure S2). Peptide **16**, however, was not active, indicating that the backbone is involved in some undefined interaction or the termini functionality is critical for binding. Analysis of the BRCT(BRCA1)–peptide crystal structure suggested the latter, which led us to generate peptides **17–19** with changes to the termini of the pSPTF peptide **1**.

**Modification to the pSXXF Termini.** Peptide **17** without the acetyl protecting group on the  $\alpha$ N of pSer and peptide **18** with an isosteric replacement of  $-\text{CONH}_2$  with  $-\text{COOH}$  at the P + 3 Phe residue were synthesized to probe the termini contribution to BRCT–peptide binding. Removal of the acetyl group in peptide **17** resulted in a  $\sim 2$ -fold loss of activity. Interestingly, the replacement of  $-\text{CONH}_2$  with  $-\text{COOH}$  (peptide **18**) resulted in a  $\sim 5$ -fold increase in activity. A possible salt bridge with the Arg<sub>1699</sub> on the BRCT(BRCA1) could be responsible for the increased activity.<sup>19</sup> Since peptide pSPVF **7** showed marginal improvement compared to peptide **1**, peptide **19** was generated with the carboxylic acid at the C-terminus of pSPVF. As hypothesized, peptide **19** also showed  $\sim 3$ -fold improvement in activity compared to peptide **1**, suggesting the possible salt bridge proposed above as a potential contact. This observation can be exploited during inhibitor design, and carboxylic acid mimics incorporated into the C-terminus of this peptide are currently under investigation.

**Isothermal Titration Calorimetry (ITC).** Direct binding experiments using ITC were conducted to determine the dissociation constants ( $K_d$ ) and the thermodynamic parameters ( $\Delta G$ ,  $\Delta H$ , and  $\Delta S$ ) of a subset of peptides listed in Table 1. A correlation with  $R^2 = 0.9$  between the  $\text{IC}_{50}$  obtained from the competitive FP assay and the  $K_d$  obtained from the binding studies using ITC (Supporting Information Figure S3) was observed. A thermodynamic optimization plot (TOP) has been suggested as an analysis method for the optimization of drug candidates by dissecting the enthalpic and entropic contributions associated with each chemical modification.<sup>20</sup> A TOP was generated using the thermodynamic parameters (Figure 2) for a subset of peptides containing a single change compared to the parent peptide **1**. Each region of the TOP is associated with some change in the thermodynamic signature of the binding event. The thermodynamic components of binding of each region are as follows: (a) For regions I and II, binding entropy is more favorable while the enthalpy is less favorable. In region I the entropic gain is greater than the enthalpic loss, resulting in a net gain in binding affinity. (b) For region III, there is loss in enthalpy and entropy. (c) For region IV, enthalpy is more favorable but not sufficient to overcome the associated loss in entropy. (d) For region V, enthalpy gains are able to overcome the entropy loss. (e) For region VI, enthalpy and entropy are favorable.

The enthalpic gain of peptide **3** is not sufficient to overcome the entropic loss, resulting in a lower binding affinity compared to peptide **1**. The enthalpic loss associated with the modifications

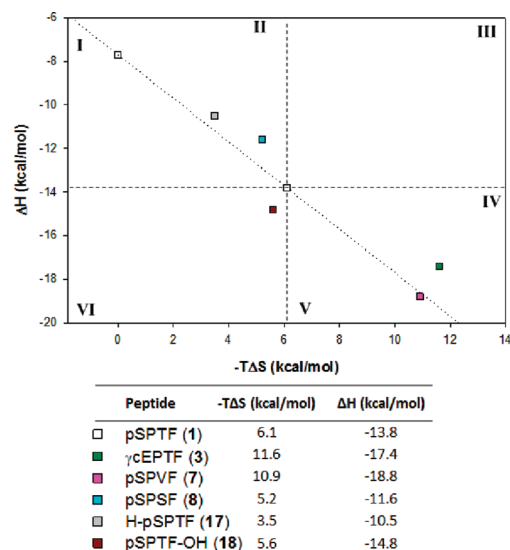


**Figure 2.** Thermodynamic optimization plot (TOP). The optimization line was generated using two experimental data points ( $-T\Delta S$ ,  $\Delta H$ ) and (0,  $\Delta G$ ) for peptide **1**. Horizontal and vertical lines were drawn through the ( $-T\Delta S$ ,  $\Delta H$ ) data point of peptide **1** to establish the six regions labeled I–VI. Peptides that fall in regions I, V, and VI result in the gain of binding affinity, while those that fall in regions II, III, and IV result in loss of binding affinity.

of peptides **8** and **17** is not offset by the entropic gain leading to slightly reduced binding affinity. Peptide **7** has a slightly higher binding affinity, as the enthalpic gain is greater than the entropic loss. Finally, peptide **18** shows an enthalpic and an entropic gain. This profile explains the increase in binding affinity of peptide **18** compared to peptide **1**. From the TOP analysis, we conclude (a) the  $\beta$ -branching with the Val<sub>(P+2)</sub> substitution in peptide **7** results in an enthalpic gain derived from the hydrophobic contact with the Glu<sub>1698</sub> side chain on BRCT. This gain is sufficient to offset the entropic loss due to the lack of a previously described intramolecular hydrogen bond in peptide **8**.<sup>17</sup> (b) The carboxylic acid at the C-terminus in peptide **18** is a significant contributor to this interaction, as an enthalpic and entropic gain is observed with this substitution.

**Thermodynamics of the BRCT(BRCA1)–pSPXF Interactions.** The origin of the differential BRCT(BRCA1) affinities of the pSPXF– $\text{CONH}_2$  and  $-\text{CO}_2\text{H}$  peptide pairs (**1** and **18**, **7**, and **19**) (see Supporting Information Table S1) has been dissected using the thermodynamic signatures derived from ITC. The similar thermodynamic profile in all four tetrapeptides (**1**, **7**, **18** and **19**, Figure 3) suggests that the binding is anchored by pS and F contacts, consistent with reported studies of the longer peptides.<sup>17,24</sup>

Peptides **18** and **19** with the carboxylic acid terminus display higher binding affinity than the carboxamide peptides **1** and **7**. More importantly, the binding affinity of the tetrapeptide **18** Ac-pSPTF- $\text{CO}_2\text{H}$  ( $K_d = 0.19 \pm 0.03 \mu\text{M}$ ) is now comparable to the decapeptide Ac-SRSTpSPTFNK- $\text{CONH}_2$  ( $K_d = 0.44 \pm 0.06 \mu\text{M}$ , our data)<sup>17</sup> and the recently reported 13-mer peptide ISRSTpSPTFNKQT ( $K_d = 0.41 \pm 0.02 \mu\text{M}$ ).<sup>24</sup> A crude extrapolation of this result suggests that Abraxas (mimicked by peptide **18**), a BRCA1 binding partner with the pSPTF motif at the C-terminus, probably binds BRCT(BRCA1) with a higher affinity compared to BACH1 (mimicked by the 13-mer peptide),

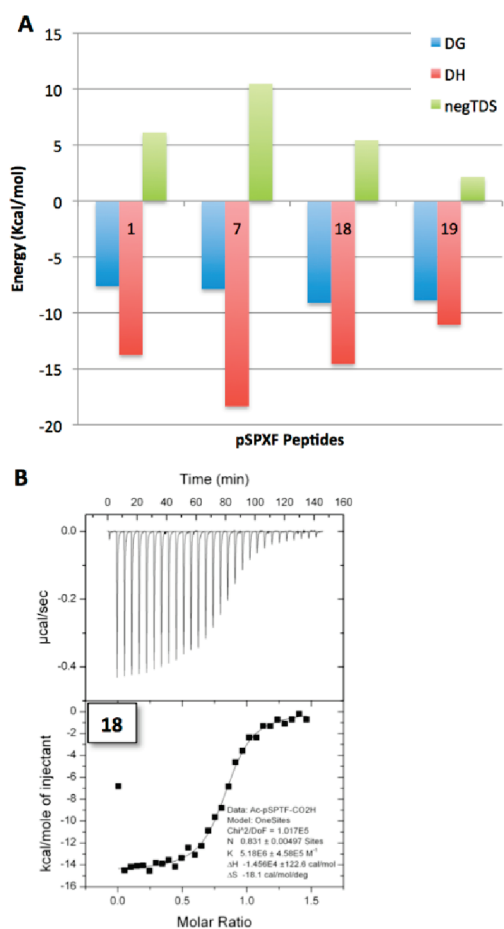


**Figure 3.** (A) Graphical representation of the thermodynamic parameters of the pSPXF peptides. (B) Representative binding isotherm of peptide 18.

another BRCA1 binding partner, with the pSPTF motif in the middle of the protein.

Calorimetric titrations at different temperatures (298–310 K; see Supporting Information Table S1 and Figure S4 for the raw data and binding isotherms, respectively) were performed to probe the effect of temperature on the binding energetics of Ac-pSPTF-CONH<sub>2</sub> and Ac-pSPTF-CO<sub>2</sub>H. Linear Van't Hoff plots (eq 1) for peptides 1 and 18 (Supporting Information Figure S5A) yield  $\Delta H_{\text{VH}}$  of  $-14.24 \pm 1.26$  and  $-16.45 \pm 3.25$  kcal, respectively. This analysis shows that the  $-\text{CO}_2\text{H}$  modification in peptide 18 results in a  $\sim 1\text{--}2$  kcal enthalpy driven binding event.

$$\ln K_d = -\Delta H/(RT) + \Delta S/R \quad (1)$$

$$\Delta C_p = d\Delta H/dT \quad (2)$$

The change in heat capacity at constant pressure,  $\Delta C_p$ , for the BRCT-tetrapeptide complex formation was determined using the standard thermodynamic relationship (eq 2). The heat capacities for the tetrapeptides 1 and 18 were calculated from the slopes of the plot of  $\Delta H$  as a function of temperature (Supporting Information Figure S5B,C). The  $\Delta C_p$  values (Ac-pSPTF-CONH<sub>2</sub>,  $-303 \pm 27$  cal mol<sup>-1</sup> K<sup>-1</sup>; Ac-pSPTF-CO<sub>2</sub>H,  $-350 \pm 69$  cal mol<sup>-1</sup> K<sup>-1</sup>) of both peptides are comparable, suggesting similar binding modes. These values are also comparable to the previously reported value for the 13-mer peptide

(ISRSTpSPTFNKQT =  $-340 \pm 30$  cal mol<sup>-1</sup> K<sup>-1</sup>),<sup>24</sup> further establishing that the tetrapeptide is the minimal unit required for BRCT(BRCA1)-peptide binding.

## CONCLUSION

A systematic SAR study was carried out, indicating the following: (a) at least three oxygen atoms are required to make the hydrophilic contact, and the side chain of Thr<sub>1700</sub> on BRCT(BRCA1) makes this binding site specific for pSer; (b) the conformationally constraining residue at the P + 1 position helps to correctly orient the hydrophilic and hydrophobic contacts on the protein;<sup>17</sup> (c)  $\beta$ -branching at the P + 2 position is optimal; (d) a salt bridge with Arg<sub>1699</sub> at the P + 3 position serves as an additional contact to enhance binding. This result is consistent with a structural study that reported similar findings.<sup>19</sup> We have identified tetrapeptides 18 and 19 with nanomolar binding affinity for BRCT(BRCA1) and have shown that their thermodynamic signatures are identical to longer peptides. These peptides will serve as leads for optimization for future BRCT(BRCA1) inhibitors.

## EXPERIMENTAL METHODS

**Peptide Synthesis.** The peptides were synthesized using standard Fmoc chemistry in-house or at the Tufts peptides core. The peptides were synthesized on Rink amide NovaGel resin (0.25 mmol) (EMD, Gibbstown, NJ) using *N*- $\alpha$ -Fmoc-protected amino acids (EMD, Gibbstown, NJ) or unnatural *N*- $\alpha$ -Fmoc protected amino acids (3B Scientific Corporation, Libertyville, IL, or Fischer Scientific, Pittsburgh, PA) and TBTU-HOBt coupling chemistry on a Focus XC synthesizer (Aapptec, Louisville, KY). Fmoc acid (5 equiv) and TBTU/HOBt (4 equiv) (Chem-Impex International, Inc., Wood Dale, IL) were dissolved in 2–3 mL of NMP. DIEA (Sigma, St. Louis, MO) (15 equiv) was added to mixture and incubated for 5 min. This mixture was then added to Fmoc-protected peptide resin and allowed to couple for 1 h. Each coupling step was monitored using the Kaiser test (Sigma, St. Louis, MO). To avoid derivatives with deletion, after the coupling step the N-terminal extremities were capped with a 5% acetic anhydride (Sigma, St. Louis, MO), 5% DIEA, 5% HOBt, and 85% NMP. After each coupling and deprotection step, the resin was thoroughly washed with DMF, MeOH, and DCM. At the end of the synthesis, the N-terminus of the desired peptide was acetylated as described above. The peptides were then cleaved from the resin using trifluoroacetic acid (TFA) (Sigma, St. Louis, MO)/TIS (Sigma, St. Louis, MO)/water (95:2.5:2.5) over a 3 h period. The crude peptides were precipitated in cold ether and air-dried overnight. Purification was performed on a preparative Agilent LC system (Agilent Technologies, Santa Clara, CA) using an Agilent C18 reverse-phase column Zobrax 300SB-C18 (21.2 mm  $\times$  150 mm, 5  $\mu$ m). Buffer A was water with 0.05% TFA, and buffer B was acetonitrile with 0.05% TFA. Gradient was buffer B from 5% to 40% in 20 min, then 40% to 100% in 5 min at 20 mL/min flow rate. The peptide fractions were lyophilized on a Sharp Freeze-110 (Aapptec, Louisville, KY). The purity of the peptides were determined by HPLC analysis with a Agilent C18 reverse phase column (4.6 mm  $\times$  50 mm, 3.5  $\mu$ m) with similar buffers but a gradient from 5% to 50% B in 20 min and a gradient from 50% to 100% B in 5 min with a 1 mL/min flow rate. Electrospray mass spectrometry was carried out on an Agilent HPLC-MS system. Amino acid analyses were performed on a model Hitachi L-8800 amino acid analyzer.

**Fluorescence Polarization Assay.** The assays were carried out in 384-well low volume Corning plates. The polarization and fluorescence were measured on a Spectramax M5 (Molecular Devices) plate reader. The peptides were titrated into a mixture of protein (1000 nM) and fluorescently labeled tetrapeptide (100 nM). The data were processed using SigmaPlot 11.0, and the IC<sub>50</sub> values were determined by nonlinear least-squares fitting.

**Isothermal Titration Calorimetry.** A Microcal VP-ITC instrument was used to measure heat changes arising from the protein–peptide interaction. All experiments were carried out at 25 °C (except the temperature dependent studies). The protein was dialyzed three times for 2 h each, and the buffer after the third dialysis was used to fill the reference cell and to dissolve the peptides (50 mM KH<sub>2</sub>PO<sub>4</sub>, pH 7.2). All solutions were degassed with stirring for 10 min using the Thermovac and filtered through a 2 μm filter before loading into syringe or cell. The peptides (100–400 μM) were loaded in the syringe, and the cell was charged with the protein (10–20 μM). The first injection of 3 μL of peptide into protein was followed by 29 injections of 10 μL/injection every 3 min. The solution was constantly stirred at 307 rpm. Dilution curves were obtained by titrating the peptide into buffer under similar conditions. This curve was subtracted from the sample curve to get the corrected heats obtained for the reaction. The data obtained were integrated using Origin 7 software supplied with the Microcal instrument.

## ■ ASSOCIATED CONTENT

**S Supporting Information.** Thermodynamic parameters used for analysis; LC and mass spectra of the peptides. This material is available free of charge via the Internet at <http://pubs.acs.org>.

## ■ AUTHOR INFORMATION

### Corresponding Author

\*Phone: (402) 559-3793. Fax: (402) 559-8270. E-mail: [anatarajan@unmc.edu](mailto:anatarajan@unmc.edu)

## ■ ACKNOWLEDGMENT

This project was supported in part by NIH Grant T32CA009476 (E.K.), Alberta Cancer Board Grant G218000116, and NIH Grant R01CA127239. We thank the members of the Natarajan lab for helpful discussions.

## ■ ABBREVIATIONS USED

BRCA1, breast cancer susceptibility gene 1; BRCT, BRCA1 carboxy terminal; HTS, high throughput screening; BACH1, BRCA1 associated carboxy helicase 1; FP, fluorescence polarization; ITC, isothermal titration calorimetry; SAR, structure–activity relationship; TOP, thermodynamic optimization plot; PPII, poly-L-proline type II

## ■ REFERENCES

- (1) Spring, D. R. Chemical genetics to chemical genomics: small molecules offer big insights. *Chem. Soc. Rev.* **2005**, *34*, 472–482.
- (2) Arkin, M. R.; Wells, J. A. Small-molecule inhibitors of protein–protein interactions: progressing towards the dream. *Nat. Rev. Drug Discovery* **2004**, *3*, 301–317.
- (3) Berg, T. Small-molecule inhibitors of protein–protein interactions. *Curr. Opin. Drug Discovery Dev.* **2008**, *11*, 666–674.
- (4) Oltersdorf, T.; Elmore, S. W.; Shoemaker, A. R.; Armstrong, R. C.; Augeri, D. J.; Belli, B. A.; Bruncko, M.; Deckwerth, T. L.; Dinges, J.; Hajduk, P. J.; Joseph, M. K.; Kitada, S.; Korsmeyer, S. J.; Kunzer, A. R.; Letai, A.; Li, C.; Mitten, M. J.; Nettlesheim, D. G.; Ng, S.; Nimmer, P. M.; O'Connor, J. M.; Oleksijew, A.; Petros, A. M.; Reed, J. C.; Shen, W.; Tahir, S. K.; Thompson, C. B.; Tomaselli, K. J.; Wang, B.; Wendt, M. D.; Zhang, H.; Fesik, S. W.; Rosenberg, S. H. An inhibitor of Bcl-2 family proteins induces regression of solid tumours. *Nature* **2005**, *435*, 677–681.
- (5) Shakespeare, W.; Yang, M.; Bohacek, R.; Cerasoli, F.; Stebbins, K.; Sundaramoorthi, R.; Azimioara, M.; Vu, C.; Pradeepan, S.; Metcalf, C., 3rd; Haraldson, C.; Merry, T.; Dalgarno, D.; Narula, S.; Hatada, M.;

Lu, X.; van Schravendijk, M. R.; Adams, S.; Violette, S.; Smith, J.; Guan, W.; Bartlett, C.; Herson, J.; Iulicci, J.; Weigele, M.; Sawyer, T. Structure-based design of an osteoclast-selective, nonpeptide src homology 2 inhibitor with in vivo antiresorptive activity. *Proc. Natl. Acad. Sci. U.S.A.* **2000**, *97*, 9373–9378.

(6) Huen, M. S.; Sy, S. M.; Chen, J. BRCA1 and its toolbox for the maintenance of genome integrity. *Nat. Rev. Mol. Cell Biol.* **2010**, *11*, 138–48.

(7) Yu, X.; Chini, C. C.; He, M.; Mer, G.; Chen, J. The BRCT domain is a phospho-protein binding domain. *Science* **2003**, *302*, 639–642.

(8) Manke, I. A.; Lowery, D. M.; Nguyen, A.; Yaffe, M. B. BRCT repeats as phosphopeptide-binding modules involved in protein targeting. *Science* **2003**, *302*, 636–639.

(9) Williams, R. S.; Lee, M. S.; Hau, D. D.; Glover, J. N. Structural basis of phosphopeptide recognition by the BRCT domain of BRCA1. *Nat. Struct. Mol. Biol.* **2004**, *11*, 519–525.

(10) Shiozaki, E. N.; Gu, L.; Yan, N.; Shi, Y. Structure of the BRCT repeats of BRCA1 bound to a BACH1 phosphopeptide: implications for signaling. *Mol. Cell* **2004**, *14*, 405–412.

(11) Clapperton, J. A.; Manke, I. A.; Lowery, D. M.; Ho, T.; Haire, L. F.; Yaffe, M. B.; Smerdon, S. J. Structure and mechanism of BRCA1 BRCT domain recognition of phosphorylated BACH1 with implications for cancer. *Nat. Struct. Mol. Biol.* **2004**, *11*, 512–518.

(12) Botuyan, M. V.; Nomine, Y.; Yu, X.; Juranic, N.; Macura, S.; Chen, J.; Mer, G. Structural basis of BACH1 phosphopeptide recognition by BRCA1 tandem BRCT domains. *Structure* **2004**, *12*, 1137–1146.

(13) Varma, A. K.; Brown, R. S.; Birrane, G.; Ladias, J. A. Structural basis for cell cycle checkpoint control by the BRCA1-CtIP complex. *Biochemistry* **2005**, *44*, 10941–10946.

(14) Shen, Y.; Tong, L. Structural evidence for direct interactions between the BRCT domains of human BRCA1 and a phospho-peptide from human ACC1. *Biochemistry* **2008**, *47*, 5767–5773.

(15) Lokesh, G. L.; Rachamalla, A.; Kumar, G. D.; Natarajan, A. High-throughput fluorescence polarization assay to identify small molecule inhibitors of BRCT domains of breast cancer gene 1. *Anal. Biochem.* **2006**, *352*, 135–141.

(16) Simeonov, A.; Yasgar, A.; Jadhav, A.; Lokesh, G. L.; Klumpp, C.; Michael, S.; Austin, C. P.; Natarajan, A.; Inglese, J. Dual-fluorophore quantitative high-throughput screen for inhibitors of BRCT-phospho-protein interaction. *Anal. Biochem.* **2008**, *375*, 60–70.

(17) Lokesh, G. L.; Muralidhara, B. K.; Negi, S. S.; Natarajan, A. Thermodynamics of phosphopeptide tethering to BRCT: the structural minima for inhibitor design. *J. Am. Chem. Soc.* **2007**, *129*, 10658–10659.

(18) Joseph, P. R.; Yuan, Z.; Kumar, E. A.; Lokesh, G. L.; Kizhake, S.; Rajarathnam, K.; Natarajan, A. Structural characterization of BRCT-tetrapeptide binding interactions. *Biochem. Biophys. Res. Commun.* **2010**, *393*, 207–210.

(19) Campbell, S. J.; Edwards, R. A.; Glover, J. N. Comparison of the structures and peptide binding specificities of the BRCT domains of MDC1 and BRCA1. *Structure* **2010**, *18*, 167–176.

(20) Freire, E. A thermodynamic approach to the affinity optimization of drug candidates. *Chem. Biol. Drug Des.* **2009**, *74*, 468–472.

(21) Zhang, R.; Madalengoitia, J. S. Conformational stability of proline oligomers. *Tetrahedron Lett.* **1996**, *37*, 6235–6238.

(22) Zhang, R.; Nickl, C. K.; Mamai, A.; Flemer, S.; Natarajan, A.; Dostmann, W. R.; Madalengoitia, J. S. Poly-L-proline type II peptide mimics as probes of the active site occupancy requirements of cGMP-dependent protein kinase. *J. Pept. Res.* **2005**, *66*, 151–159.

(23) Zhou, N.; Luo, Z.; Luo, J.; Fan, X.; Cayabyab, M.; Hiraoka, M.; Liu, D.; Han, X.; Pesavento, J.; Dong, C. Z.; Wang, Y.; An, J.; Kaji, H.; Sodroski, J. G.; Huang, Z. Exploring the stereochemistry of CXCR4-peptide recognition and inhibiting HIV-1 entry with D-peptides derived from chemokines. *J. Biol. Chem.* **2002**, *277*, 17476–17485.

(24) Nomine, Y.; Botuyan, M. V.; Bajzer, Z.; Owen, W. G.; Caride, A. J.; Wasielewski, E.; Mer, G. Kinetic analysis of interaction of BRCA1 tandem breast cancer C-terminal domains with phosphorylated peptides reveals two binding conformations. *Biochemistry* **2008**, *47*, 9866–9879.